Speed detection to suppress motion artifacts (MA) in laser speckle contrast imaging (LSCI)

Ata Chizari*[a], Mirjam J. Schaap[b], Tom Knop[a], Marieke M.B. Seyger[b], Wiendelt Steenbergen[a],
[a] Biomedical Photonic Imaging, Technical Medical Centre, Faculty of Science and Technology, University of Twente, PO Box 217, 7500 AE Enschede, The Netherlands;
[b] Department of Dermatology, Radboud University Medical Center, P.O. Box 9101, 6500 HB Nijmegen, The Netherlands;

*a.chizari@utwente.nl; https://people.utwente.nl/a.chizari

ABSTRACT

Laser speckle contrast imaging (LSCI) is an optical technique for noninvasive assessment of microcirculatory blood flow. LSCI has a broad application in medicine including dermatology. Since laser speckles are the basis for this imaging modality, any external motions during a measurement from both patient and operator affect the blood flow images. This challenge is called motion artefacts (MA). Here, we propose a complete procedure for analysis of speckles, that is, pre-segmentation, segmentation, motion detection, spatial alignment, perfusion map calculation and MA suppression. The handheld perfusion imager (HAPI) operated in both handheld and mounted schemes, has been used for measurements on 14 psoriasis subjects. The advantage of HAPI is use of a single monochromatic camera for both speckle imaging and motion detection. We make use of the black marker dots (made by the clinical investigator to determine visual psoriasis lesion boundary) for calculation of two-dimensional displacements of HAPI during each measurement (i.e. on-surface displacements). These on-surface displacements are integrated to translate each speckle image back to the initial position at the start of the measurement (i.e. spatial alignment). Furthermore, in handheld measurements, MA corrected blood flow maps (also called perfusion maps) are formed by extrapolation of a linear fit from local perfusion versus detected speed to the zero speed, that is, a value ideally always lower than the local mean perfusion. We show that our MA suppression technique makes handheld perfusion maps more similar to the associated mounted perfusion maps in term image histograms and mean values.

Keywords: laser speckle contrast imaging, motion artefacts, psoriasis, handheld device, mean separation segmentation, enhanced correlation coefficient maximization, spatial alignment, linear fit extrapolation.

1. INTRODUCTION

Skin perfusion can be noninvasively evaluated by an optical technique called laser speckle contrast imaging (LSCI). When a laser source illuminates a scattering medium such as human tissue, light rays undergo different pathlengths. When backscattered laser light from such scattering medium is imaged on a camera, an interference pattern will be formed called speckle. The dynamic nature of the medium due to for instance blood flow, results in the formation of dynamic speckle patterns. When imaged by a certain exposure time, the dynamic speckles will be integrated and a so called blurred speckle pattern will be formed. A criterion to quantify such blurred speckle pattern is its spatial normalized standard deviation (speckle contrast) such that the higher the blood flow the more blurred the speckle pattern and the lower the speckle contrast. This forms the basis of LSCI.

Since the first introduction of LSCI in 1980s[1], it is still an active field of study and becomes advanced in different aspects. A theoretical basis has been introduced to increase robustness of LSCI to overexposure which is an important optical setup parameter[2]. Computational three-dimensional blood flow reconstruction with high spatiotemporal resolution has been realized based on Mote Carlo simulation which is of need in functional neural imaging[3]. To realize preclinical diagnosis such as point-of-care endoscopy, a handheld LSCI endoscope using an off-the-shelf smart-phone has been made[4]. Also, the wireless perfusion imager (WIPI) has been developed with intraoperative application[5]. As a potential alternative to the time-consuming procedure of manual annotation in perfusion images, deep learning has been employed on LSCI data for prognosis prediction and evaluation of keloids[6]. Apart from the conventional speckle contrast calculation, vision-based optical flow algorithms have been used not only to enhance spatiotemporal resolution, but also to facilitate quantitative estimation of blood flow[7] and non-rigid registration of perfusion images prior to temporal averaging[8]. Also, a

Optical Coherence Imaging Techniques and Imaging in Scattering Media V, edited by Benjamin J. Vakoc, Maciej Wojtkowski, Yoshiaki Yasuno, Proc. of SPIE Vol. 12632, 1263213
 · 0277-786X · doi: 10.1117/12.2672211

parameter fitting procedure based on highspeed imaging has been introduced that operates on speckle intensity correlation function in order to accurately predict relative perfusion[9]. Recently, LSCI has been employed in a wide range of medical applications including ophthalmology[10], neurology (brain)[11], robot-assisted surgery[12], dermatology (psoriasis)[13] and plastic surgery[14].

The rather simple and affordable hardware required for LSCI enables its handheld use which brings many advantages such as compactness and operator-friendliness[15]. However, the perfusion maps obtained by LSCI are affected by motion artifacts (MA) due to the sensitivity of speckles to any source of movements including subject and operator. So far, this challenge has been addressed in different ways. The MA studies can be categorized in mounted and handheld modalities. In mounted modality, placing a static object in the field-of-view (FOV) such as an adjacent opaque surface[16] and a bilayer adhesive[17] has been explored. Also, places in a speckle image where speckle contrast was independent of blood flow was explored in order to regress out MA data[18]. Optical flow motion tracking was applied to correct for non-rigid movements in speckle image series[8]. Controlled motorized experiments were carried out to address MA in multi-exposure case[19] and the speckle contrast drop caused by translation of the system has been analytically modelled[20]. Dual-wavelength scheme has been shown to suppress MA-related signals from the measurements[21].

In handheld modality, static objects within the FOV such as a fiducial marker[22] have been used, too. Hardware modifications such as a motorized image stabilizer[23] or spherical\planar wave illumination[24] improve robustness of LSCI systems against MA. Translational motions of the LSCI system with respect to the test object has been theoretically modelled[25] and validated[26]. Vision-based methods such as segmentation and image alignment have shown promises in creating handheld blood flow maps that are comparable with mounted pairs[27]. In a previous study, we introduced a method to suppress motion artifacts based on extrapolation of the speed vectors which are calculated by tracking markers on speckle images directly[28]. In this study, we elaborate on the theory of this MA suppression method and analyse its performance in 14 pairs of handheld/mounted measurements operated on psoriasis subjects.

2. THEORY

Consider the laser beam on the $x-y$ surface moving at velocity

$$\vec{v} = v_x(t)\vec{x} + v_y(t)\vec{y}. \tag{1}$$

The absolute speed will be calculated as $V(t) = \sqrt{v_x^2 + v_y^2}$. The speckle contrast is shown to be a function of exposure time T and correlation time τ_c as[29]

$$C^2 = \frac{\tau_c}{2T}\left[2 - \frac{\tau_c}{T}\left(1 - \exp\left(-\frac{2T}{\tau_c}\right)\right)\right]. \tag{2}$$

The perfusion index v_c can also be approximated to be an inverse function of the correlation time as[29] $v_c = \lambda/(2\pi\tau_c)$. Therefore, v_c can be interpolated from a measured C via a prepared numerical lookup table. In an MA-free system, the resulted time-averaged v_c corresponds to the tissue perfusion; however, what is measured in practice would be

$$v_c' = m(x,y)V(t) + \widehat{v_c}(x,y), \tag{3}$$

where m is the space-dependent fraction of applied speed and $\widehat{v_c}$ is the MA-free perfusion index as an estimation of the time-integrated perfusion obtained in mounted mode which is calculated as

$$\overline{v_c} = \int_0^{T_m} v_c(x,y,t)dt, \tag{4}$$

where T_m is the measurement time. Thus, the goal is to define $\widehat{v_c}(x,y)$ and compare it with the ground truth $\overline{v_c}\ (x,y)$. Note that the time-integrated perfusion in handheld mode without correction would be $\overline{v'_c} = \int_0^{T_m} v'_c(x,y,t)dt$.

3. METHODS AND MATERIALS

A detailed description of the used handheld perfusion imager (HAPI, Figure 1(a, bottom)), the measurement protocol, and the data analysis have been provided in Chizari et al.[27,28]. Briefly, light of a laser source ($\lambda = 671$ nm) has been coupled to a single mode fiber. At the distal end of the fiber on the handheld probe, the laser light has been expanded using a lens in order to create spherical wave illumination. The monochromatic camera meant for speckle imaging was equipped with

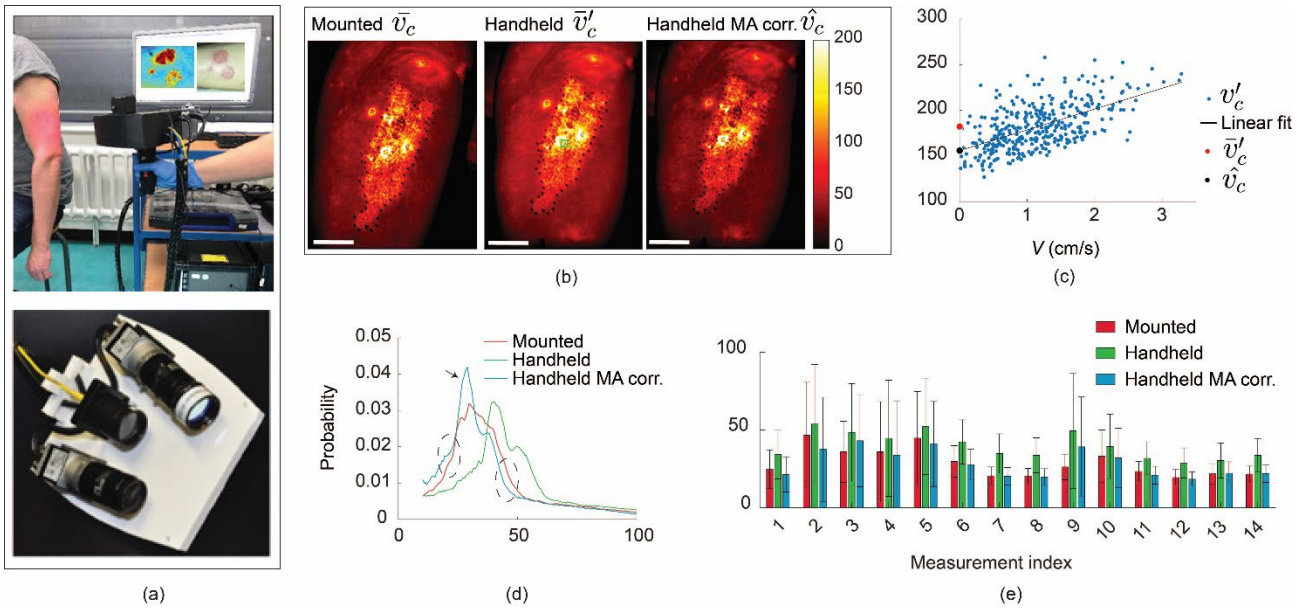

Figure 1 (a, top), A photograph of a representative handheld measurement on a psoriasis subject reprinted from Schaap et al.[30]. (a, bottom), Handheld perfusion imager (HAPI) probe with an opened casing reprinted from Chizari et al.[31]. Comparison of (b, left) mounted measurement index 5 with (b, middle) the handheld pair and (b, right) the corresponding motion artefact corrected (MA corr.) image. Green square in (b, middle) refers to the location where data of (c) come from. Scale bars, 2.5 cm. (c) Perfusion versus on-surface speed of a handheld measurement for a square region (4.2 mm side dimension) shown in green in (b, middle). $\bar{v}_c$ represents average perfusion value. $v_c(v = 0)$ represents y-intercept of the fitted line (i.e. zero-speed extrapolated point) as a compensation value. (d) Probability density functions of the perfusion images shown in (b). Dashed ellipses indicate the closeness of the MA corr. case to the mounted case. Black arrow shows the perfusion area for which over-compensation has been resulted. (e) Overview of the 14 measurements. Data are mean±std of the entire perfusion maps which results in a rather high std value per bar value.

a linear polarizer and a bandpass filter centered around the laser wavelength. The working distance was 30 cm from the front size of the probe, the camera frame rate was set as 50 Hz and the exposure time was $T = 10$ ms. Each measurement included 7 seconds camera recording during which room lighting was switched off. Psoriasis subjects refrained from caffeine, nicotine and intense physical activity prior to each measurement. The HAPI probe was placed on a tripod for mounted measurements; and the operator kept the probe normally (i.e. without overconcentration) and in a convenient manner during the handheld measurements (see Figure 1(a, top)). The acquired speckle frame underwent pre-segmentation, segmentation, speed detection and spatial alignment. Then, the perfusion frames were created to obtain $v'_c(x, y, t)$ and the speed values $V(t)$ were calculated from the detected displacements on x and y directions.

4. RESULTS

In Figure 1(b) representative averaged perfusion images have been shown. The boundaries of the psoriasis lesion have been marked by the clinical investigator for follow-up purposes. The lesion area is inhomogeneously of higher perfusion compared to the background area (i.e. the healthy skin). On a visual basis, the handheld case has higher values compared to the mounted due to MA. The goal is to suppress the velocity term shown in (3) such that handheld case resembles the mounted case; to be specific, reliable enough to be used by the clinical investigator for perfusion assessment.

To perform the MA suppression, a square window scanned the stack of spatially aligned handheld perfusion images $v'_c(x, y, t)$ with a step size the same as the window size. At each location, the estimated $\hat{v}_c(x, y)$ was calculated to form the resulted MA corrected image shown in Figure 1(b, right). As an example of the linear fitting and extrapolation, see Figure 1(c) which is the corresponding data of the green window (side dimension of 50 pixels) shown in Figure 1(b, middle).

To analyse the performance of the proposed method, first, a high-pass threshold of 10 perfusion units was applied to all perfusion images in order to bypass irrelevant image background. Then, normalized probability density functions of the three images per measurement index were made. Figure 1(d) depicts such density functions for the experiment index 5.

Here, the handheld case is shifted to the right (higher perfusion values due to MA). We can see that the MA corrected curve approaches the mounted case (see the dashed ellipses). On the other hand, a peak around 30 perfusion units has been formed which causes some deviation from the ground truth (mounted).

As the second phase of performance evaluation, average perfusion has been compared (Figure 1(e)). We can see that in all cases, handheld is higher than the corresponding mounted and MA corrected is lower than the corresponding handheld which are both expected. Ideally, MA corrected is desired to be the same as mounted. In some cases, MA corrected is lower than mounted which suggests occurrence of overcompensation. One explanation is the fitting inaccuracy due to the cloudiness of the data points in Figure 1(c). The cloudiness is partially resulted by the unavoidable changes in skin perfusion which is a physiological body function and partly due to the tracking error caused by the machine vision algorithm. Here, the findable textures in an image, algorithm parameters such as number of iterations, and the frame rate with respect to the frequency of movements play a role.

Also, one might question the rather high standard deviation (std) for each case. This is due to the calculation of the entire perfusion map (including lesion and healthy skin) in one time. Thus, here the std does not solely imply algorithm error. As an improvement step, each perfusion map prior to mean/std calculation could be grouped to lesion and health skin using an image masking method. Altogether, the effectiveness of the proposed method has been shown using both histogram and mean/std analysis.

5. CONCLUSION

In this paper, we introduced a motion artefact (MA) suppression method based on speed detection in laser speckle contrast imaging (LSCI) when operated handheld. This method does not require placing a static object in the field-of-view to detect MA associated speckle frames but measures the spontaneous speed to do so. Moreover, we do not exclude MA associated frames but merely suppress the MA term. The speed detection has been carried out directly on speckle images making the most of the black markers made by the clinical investigator for other purposes. Therefore, no extra hardware or material is required for MA suppression. By comparing 14 pairs of measurements on psoriasis subjects, we have analyzed the performance of this method. Another advantage of this method is that it finds the relation between the local perfusion and the applied speed and defines the MA term for each location and perfusion level; hence, it does not require information about optical properties of the media (i.e. scattering and absorption). We conclude that the proposed approach is a step towards obtaining reliable LSCI perfusion maps which is of high demand in a wide range of medical applications.

6. ETHICS DECLARATIONS

All psoriasis participants provided informed consent before enrollment. The ethics committee of the region of Arnhem-Nijmegen and the Radboud university medical center, Nijmegen, the Netherlands (NL69174.091.19) approved the use of the HAPI system and the study protocol. Relevant guidelines and regulations were applied for all experiments.

7. ACKNOWLEDGMENT

This study was supported by the Open Technology program of the Netherlands Organization for Scientific Research (NWO), Domain Applied and Engineering Sciences, under grant number 14538.

8. REFERENCES

1. Fercher, A. F. & Briers, J. D. Flow visualization by means of single-exposure speckle photography. *Opt. Commun.* **37**, 326–330 (1981).
2. Földesy, P., Siket, M., Nagy, Á. & Jánoki, I. Correction of overexposure in laser speckle contrast imaging. *Opt. Express* **30**, 21523 (2022).
3. Jafari, C. Z., Mihelic, S. A., Engelmann, S. & Dunn, A. K. High-resolution 3D Blood Flow Tomography in the Sub-diffuse Regime Using Laser Speckle Contrast Imaging. *Opt. InfoBase Conf. Pap.* **27**, 1–18 (2022).
4. Kim, Y., Choi, W. J., Oh, J. & Kim, J. K. Compact Smartphone-Based Laser Speckle Contrast Imaging Endoscope Device for Point-of-Care Blood Flow Monitoring. *Biosensors* **12**, (2022).
5. Teunissen, S. E. M. Wireless Laser Speckle Contrast Imaging during DIEP flap breast reconstruction : an evaluation of the first prototype Master Thesis Technical Medicine. (2022).
6. Li, S. *et al.* A Workflow for Computer-Aided Evaluation of Keloid Based on Laser Speckle Contrast Imaging

and Deep Learning. *J. Pers. Med.* **12**, (2022).
7. Aminfar, A. H., Davoodzadeh, N., Aguilar, G. & Princevac, M. Application of optical flow algorithms to laser speckle imaging. *Microvasc. Res.* **122**, 52–59 (2019).
8. Liu, X. *et al.* Motion correction of laser speckle imaging of blood flow by simultaneous imaging of tissue structure and non-rigid registration. *Opt. Lasers Eng.* **140**, 106526 (2021).
9. Postnov, D. D., Tang, J., Erdener, S. E., Kılıç, K. & Boas, D. A. Dynamic light scattering imaging. *Sci. Adv.* **6**, 1–10 (2020).
10. Bunke, J. *et al.* Hyperspectral and Laser Speckle Contrast Imaging for Monitoring the Effect of Epinephrine in Local Anesthetics in Oculoplastic Surgery. *Ophthal. Plast. Reconstr. Surg.* **38**, 462–468 (2022).
11. Cumsille, P., Lara, E., Verdugo-Hernández, P., Acurio, J. & Escudero, C. A robust quantitative approach for laser speckle contrast imaging perfusion analysis revealed anomalies in the brain blood flow in offspring mice of preeclampsia. *Microvasc. Res.* **144**, (2022).
12. Liu, Y. Z. *et al.* Utility and usability of laser speckle contrast imaging (LSCI) for displaying real-time tissue perfusion/blood flow in robot-assisted surgery (RAS): comparison to indocyanine green (ICG) and use in laparoscopic surgery. *Surg. Endosc.* (2022) doi:10.1007/s00464-022-09590-3.
13. Margouta, A. *et al.* Blunted Microvascular Reactivity in Psoriasis Patients in the Absence of Cardiovascular Disease, as Assessed by Laser Speckle Contrast Imaging. *Life* **12**, 1796 (2022).
14. To, C. *et al.* Intraoperative Tissue Perfusion Measurement by Laser Speckle Imaging: A Potential Aid for Reducing Postoperative Complications in Free Flap Breast Reconstruction. *Plast. Reconstr. Surg.* **143**, 287e-292e (2019).
15. Chizari, A. Handheld laser speckle contrast perfusion imaging. (University of Twente, 2021). doi:10.3990/1.9789036552394.
16. Mahé, G. *et al.* Laser speckle contrast imaging accurately measures blood flow over moving skin surfaces. *Microvasc. Res.* **81**, 183–188 (2011).
17. Omarjee, L. *et al.* Optimisation of movement detection and artifact removal during laser speckle contrast imaging. *Microvasc. Res.* **97**, 75–80 (2015).
18. Guilbert, J. & Desjardins, M. Movement correction method for laser speckle contrast imaging of cerebral blood flow in cranial windows in rodents. *J. Biophotonics* e202100218 (2021).
19. Amphan, D. Quantification and Detection of Motion Artifacts in Laser Speckle Contrast Imaging. (2022).
20. Chizari, A., Tsong, W., Knop, T. & Steenbergen, W. Modeling movement artefacts in handheld laser speckle contrast perfusion imaging: influence of wavefront types. in *Dynamics and Fluctuations in Biomedical Photonics XIX* (eds. Tuchin, V. V., Leahy, M. J. & Wang, R. K.) vol. 1195905 13 (SPIE, 2022).
21. Heeman, W. *et al.* Real-time, multi-spectral motion artefact correction and compensation for laser speckle contrast imaging. *Sci. Rep.* **12**, 1–9 (2022).
22. Lertsakdadet, B. *et al.* Correcting for motion artifact in handheld laser speckle images. *J. Biomed. Opt.* **23**, 36006 (2018).
23. Lertsakdadet, B., Dunn, C., Bahani, A., Crouzet, C. & Choi, B. Handheld motion stabilized laser speckle imaging. *Biomed. Opt. Express* **10**, 5149 (2019).
24. Chizari, A., Knop, T., Tsong, W., Schwieters, S. & Steenbergen, W. Influence of wavefront types on movement artefacts in handheld laser speckle contrast perfusion imaging. *OSA Contin.* **4**, 1875 (2021).
25. Chizari, A., Tsong, W., Knop, T. & Steenbergen, W. Modelling movement artefacts in handheld laser speckle contrast imaging. in *Dynamics and Fluctuations in Biomedical Photonics XX* (eds. Zalevsky, Z., Tuchin, V. V., Leahy, M. J. & Wang, R. K.) vol. 1237804 8 (SPIE, 2023).
26. Chizari, A., Tsong, W., Knop, T. & Steenbergen, W. Prediction of motion artifacts caused by translation in handheld laser speckle contrast imaging. *J. Biomed. Opt.* **28**, 1–17 (2023).
27. Chizari, A. *et al.* Handheld versus mounted laser speckle contrast perfusion imaging demonstrated in psoriasis lesions. *Sci. Rep.* **11**, 16646 (2021).
28. Chizari, A., Schaap, M. J., Knop, T., Seyger, M. M. B. & Steenbergen, W. Reliability of handheld laser speckle contrast perfusion imaging demonstrated in psoriasis lesions. in *Photonics in Dermatology and Plastic Surgery 2022* (eds. Choi, B. & Zeng, H.) 34 (SPIE, 2022). doi:10.1117/12.2608663.
29. Briers, J. D. Laser speckle contrast analysis (LASCA): a nonscanning, full-field technique for monitoring capillary blood flow. *J. Biomed. Opt.* **1**, 174 (1996).
30. Schaap, M. J. *et al.* Perfusion measured by laser speckle contrast imaging as a predictor for expansion of psoriasis lesions. *Ski. Res. Technol.* **28**, 104–110 (2022).

31. Chizari, A., Knop, T., Sirmacek, B., van der Heijden, F. & Steenbergen, W. Exploration of movement artefacts in handheld laser speckle contrast perfusion imaging. *Biomed. Opt. Express* **11**, 2352 (2020).